DØ Note 6339

Measurements in W+jets production at $\sqrt{s}$ =1.96 TeV

The DØ Collaboration
URL http://www-d0.fnal.gov
(Dated: June 6 2012)

We present new measurements related to jets produced in association with a W boson in proton-antiproton collisions at $\sqrt{s} = 1.96$ TeV. Differential cross-sections corrected for detector acceptance and efficiencies are presented as a function of the n^{th} jet rapidities, dijet invariant mass spectra, and W boson transverse momentum for events containing up to four identified jets. The probability of additional jet emission in $W+ \geq 2$jet events is studied as a function of dijet rapidity separations for p_T and angular-ordered jets. The measurements are compared to NLO pQCD, all-order resummation and matrix-element parton-shower matched Monte Carlo predictions.

Preliminary Results for Summer 2012 Conferences

I. INTRODUCTION

In this note we present new measurements related to jet production in inclusive $W+(n)$jet final states, with n=1-4, using 3.8 fb^{-1} of proton-antiproton collisions collected with the DØ detector [1]. These measurements follow from earlier measurements of inclusive W+jets production cross-sections and differential cross sections as a function of the n^{th} jet p_T [2] up to $n = 4$. $W+(n)$jet final states are of interest because of the important role they play in backgrounds to new physics and as multi-scale QCD processes. In the case of searches, W+jets production is dominant in several SUSY and Higgs search channels; in the case of Standard Model processes with small cross-section, like single top and Vector Boson Fusion processes are often overwhelmed by W+jets backgrounds.

These new measurements provide differential cross sections of hadronic and leptonic variables, which will provide validation of new theoretical calculational approaches and valuable input for Monte Carlo tuning. We provide measurements of n^{th} jet rapidities, (which test the modeling of parton emission, which is difficult to predict accurately in the forward region, corresponding to large values of rapidity), measurement of the W boson transverse momentum, and the dijet invariant mass in inclusive W+2jet and W+3jet events, which is an important variable for electroweak vector boson fusion (VBF) production, and for VBF Higgs searches.

In addition, the probability of additional jet emission as a function of dijet rapidity separation is studied for the first time in inclusive W+2jet events, for both p_T-ordered and rapidity-ordered jets. This variable has consequences for the design of jet vetoes in high jet multiplicity final states, which is particularly important for VBF Higgs searches and VBF electroweak production. It is also sensitive to BFKL-like effects [3, 4] when the two jets are widely separated in rapidity.

II. DATA SELECTION AND TREATMENT

These measurements uses a sample of $W \to e\nu + n$ jets candidate events corresponding to 3.8 fb^{-1} of data collected with the DØ detector in Run II of the Fermilab Tevatron Collider.

The D0 detector consists of a central tracking system, comprising a silicon microstrip tracker and a fiber tracker, in an approximately 2 T axial magnetic field. These components are used primarily to identify the location of the $p\bar{p}$ interaction vertex and the electron produced in the decay of the W boson candidate and to reconstruct charged tracks. Outside of the tracking system, a liquid-argon and uranium calorimeter is divided into a central section and two end sections that are used to identify electromagnetic and hadronic showers. A detailed description of the DØ detector can be found in Ref. [1].

The data were collected using a suite of electron and electron+jet triggers. Events were then processed through the DØ reconstruction program which identifies jet and W boson candidates. Jets are identified with the DØ RunII midpoint cone algorithm [5], which uses a cone of radius $R_{\rm cone} = 0.5$ to cluster calorimeter cells. Jets are corrected for the calorimeter response, instrumental and out-of-cone showering effects, and additional energy deposits in the calorimeter that arise from detector noise and pile-up from multiple interactions and different beam crossings. These jet energy scale corrections are determined using transverse momentum imbalance in γ + jet events, where the electromagnetic calorimeter response is calibrated using $Z/\gamma^* \to e^+e^-$ events.

Jets are required to have at least two tracks that point to their associated $p\bar{p}$ vertex, the so-called "jet-vertex confirmation", to improve the identification of the jets and ensure they are associated to the same proton anti-proton collision as the W boson under consideration. Jets are ordered in decreasing transverse momentum and we call the jet with the highest transverse momentum "leading." Electrons are identified as clusters of calorimeter cells in which 95% of the energy in the shower is deposited in the electromagnetic (EM) section. The electron candidates must be isolated from other calorimeter energy deposits, have spatial distributions consistent with those expected for electron showers, and the event must contain a reconstructed track matched to the EM shower that is isolated from other tracks. Events with a second isolated electron are removed to suppress the background from Z boson and Drell-Yan production. The missing transverse energy $\not\!\!E_T$ in the event is calculated as a vector sum of the calorimeter cell energies and is corrected for the presence of any muons. Because the longitudinal component of the momentum of the neutrino is not measured, the measured properties of the W boson candidates are limited to their transverse energy, E_T^W, and transverse mass, defined as $M_T^W = \sqrt{(\not\!\!E_T + p_T^e)^2 - (\not\!\!E_x + p_x^e)^2 - (\not\!\!E_y + p_y^e)^2}$ where p_T^e is the transverse momentum of the electron, and p_x^e and p_y^e are the x and y components of the electron's momentum.

The event selection cuts that define the kinematic region are described in Table I. Selection cuts are motivated by efficient and accurate reconstruction, and by reducing contributions to the dataset by backgrounds from other processes. These cuts strongly suppress the multijet background while maintaining high efficiency for events in which a W boson was produced. The background processes that are considered in this analysis are Z+jets, $t\bar{t}$, single top, diboson and multijet production. All background processes (and the signal process) apart from multijet production are

TABLE I: Event selection cuts.

Electron Selection	
Transverse momentum p_T	> 15 GeV
Pseudorapidity $\|\eta\|$	< 1.1
ΔR between electron and nearest jet	> 0.5
Jet Selection	
number of jets	≥ 1
Transverse energy E_T	> 20 GeV
Rapidity $\|y\|$	< 3.2
Global Selection	
z position of the primary vertex $\|z_{vtx}\|$	< 60 cm
Missing transverse energy $\not\!\!E_T$	> 20 GeV
Transverse mass $M_T(W)$	> 40 GeV

estimated using Monte Carlo samples. The relatively small multijet production is estimated using data in a multijet enriched control region. Contributions from $W(\rightarrow \tau\nu \rightarrow e\nu\nu)$+jets processes are also considered as a background and estimated using simulation.

The sum of the backgrounds are subtracted bin-by-bin from the data, leaving only W+jet (light and heavy flavor) contributions. The measured background-subtracted distributions are unfolded to particle level, correcting for acceptance and bin-to-bin migrations using the regularized matrix inversion method as implemented in GURU [6]. The analysis method and determination of systematic uncertainties is the same as that used for unfolding of the jet transverse momentum distributions in W+jet events in a previous DØ publication [2]

Unfolded phase space

We define the kinematic phase-space into which we unfold our final results by the following requirements:

- Jet transverse momentum: $p_T > 20$ GeV
- Jet rapidity: $|y| < 3.2$
- Electron transverse momentum: $p_T > 15$ GeV
- Electron pseudorapidity: $|\eta| < 1.1$
- Vector sum of all neutrino transverse momenta: $E_\nu > 20$ GeV
- Transverse mass cut: $m_T(W) > 40$ GeV

III. SYSTEMATIC UNCERTAINTIES

Systematic uncertainties due to the following sources are evaluated for each observable:

- Jet Energy Scale (JES) uncertainty,
- Jet Energy Resolution (JER),
- Jet reconstruction efficiency,
- EM-object identification,
- Uncertainties on jet vertex confirmation efficiencies,
- Trigger efficiency
- Monte Carlo background modelling uncertainties
- Unfolding uncertainties due to acceptance corrections and migration matrices
- Uncertainties on multijet background determination

Systematic uncertainties dominate over statistical uncertainties across the major part of the measured phase space. Total cancellation of the integrated luminosity uncertainty, and partial cancellations of systematic uncertainties on trigger and EM-object ID come from normalisation of the corrected results to the measured inclusive W production cross-section.

The largest uncertainties in the observables presented in this note come from Jet Energy Scale (JES) and Jet Energy Resolution (JER) uncertainties. These contribute $\sim 1-10\%$ uncertainty at high W boson p_T (dependent on jet multiplicity), and can contribute 30% or more each in the lowest p_T bins. Similarly, for dijet mass measurement these uncertainties dominate, being of order $\sim 10-15(15-20)\%$ at low mass and $\sim 6-9(10)\%$ at high mass in the inclusive two (three) jet bin. As a function of jet rapidities, JER and JES uncertainties vary significantly, rising from $\sim 4-20\%$ for central jets (dependent on jet multiplicity) to $\sim 20-35\%$ for the most forward jets studied. The jet emission probabilities benefit from additional systematic cancellations in their construction. JES and JER uncertainties remain the largest contributors to the overall uncertainty, at around $1-3\%$ at small angular separations up to 10% at wide angle. Uncertainties due to Multijet background modelling, unfolding procedure and jet vertex confirmation are also significant contributions, particularly at large rapidity intervals.

IV. THEORETICAL PREDICTIONS

Comparison is made of the corrected data distributions to a variety of theoretical calculations:

1. Matrix Element plus (Leading-Order) Parton Shower matched Monte Carlo event generator predictions from Sherpa 1.4.0 [9]
2. All-order resummation predictions from High Energy Jets (HEJ) [7]
3. Next-to-Leading-Order (NLO) Blackhat+Sherpa [8] predictions

A. Sherpa

Comparison is made to leading-order matrix element parton shower matched Monte Carlo produced with Sherpa v.1.4.0 [9], with the CT10 [10] PDF set and with the factorisation and renormalisation scales chosen as discussed in Ref. [11]. Results are provided using the DØ RunII MidPoint cone algorithm at particle-level, with cone radius $R_{\text{cone}} = 0.5$. The Sherpa default tuning parameters are used, with the exception of the MPI cutoff scale, which was tuned to fit the CDF underlying event data in Drell-Yan production [12]. Hadronisation is conducted using Sherpa's internal Cluster fragmentation approach [9]. Differential cross-section results are normalized to the inclusive W production cross-section determined in Sherpa to be 1038.6 ± 0.2 pb at particle-level (for comparison, the measurement of the inclusive W production cross-section from this experiment in the same phase space is 1132^{+81}_{-92} pb [2]).

B. High Energy Jets (HEJ)

High Energy Jets (HEJ) [4, 7] is an implementation in a parton-level Monte Carlo generator of an exclusive, all-order resummation of the perturbative contributions to production of wide angle emissions at hadron colliders. Such predictions are particularly suited for description of events containing two jets with a large rapidity separation.

Predictions are produced using the DØ RunII Midpoint cone algorithm at particle-level, with $R_{\text{cone}} = 0.5$. The factorisation and renormalisation scale is chosen to be $\mu = 2 \times \max\{\mathrm{p}_{\mathrm{T}}^{\mathrm{j}}\}$, with scale uncertainties estimated by variation around this central scale choice by up and down by a factor of two. As HEJ is capable only of describing two jet and higher multiplicity events, differential cross-sections are normalised by the measured inclusive W cross-section in order to allow a like-to-like comparison of the distributions with the data.

C. Blackhat+Sherpa NLO

The data are compared to next-to-leading (NLO) fixed order predictions from Blackhat+Sherpa [8], which are presented for W + 4jet events at the Tevatron for the first time in this note. The Blackhat+Sherpa predictions employ the renormalisation and factorisation scale choice $\mu = \mu_F = \mu_R = \frac{1}{2}\hat{H}_T$ where $\hat{H}_T$ is defined as the scalar sum of the parton and W transverse energies. Scale uncertainties are estimated by varying μ up and down by a factor

of two. The calculations use the `MSTW2008nlo68cl` PDF set [13], with values of $\alpha_s(\mu)$ set consistently with the PDF choice, using a two-loop running at NLO.

Predictions are generated with the SIScone jet algorithm applied at particle-level rather than with the DØ RunII Midpoint cone jet algorithm (for IR-safety concerns at higher jet multiplicities). The effect of changing between SIScone and DØ RunII Midpoint cone jet algorithms has been found to result in variations in the observable cross-sections of an order of magnitude smaller than the scale uncertainties on the theory, and no correction has been made to account for the difference in the jet finder algorithm between data and NLO. Results are normalised to the inclusive W production cross-section prediction at NLO [8], determined to be 1153^{+17}_{-7}, in the unfolded phase space.

Non-perturbative corrections

As NLO Blackhat predictions are provided at the parton-level and the data is corrected to the particle-level, we apply non-perturbative corrections to the theory to correct for hadronization and underlying event contributions. Non-perturbative corrections were produced using Sherpa 1.4.0. Corrections are produced from the ratio of the observed differential production cross-section derived from Sherpa at particle-level (using Sherpa's internal cluster fragmentation model) to the differential production cross-section from Sherpa at parton-level, which includes parton showering but without hadronization or multiple scattering, and with electron final state emission disabled. Uncertainties on the non-perturbative corrections are obtained by recalculating the particle-level Sherpa 1.4.0 results as described above using the Lund string fragmentation model, taking the difference between the two as a symmetric systematic uncertainty on this correction.

V. RESULTS

All results presented here are corrected to the particle-level, correcting for all detector efficiencies and resolution effects. For all results, ratio panes of Theory/Data are shown below the main result pane. All differential cross-section measurements shown in Figures 1 to 3 are normalised to the total inclusive W cross-section [2] (in the defined phase space of the measurement) in order to reduce systematic uncertainties on the measurement.

Figure 1 shows the normalised differential production cross-sections of $W + n$jet events for $n = 1 - 4$ as a function of the W boson transverse momentum in each of the inclusive jet multiplicity bins. Data uncertainties shown are the result of statistical and systematic uncertainties added in quadrature. Good agreement is seen between the data and predictions of HEJ and NLO Blackhat, in all jet multiplicity bins within uncertainties. Non-perturbative corrections to the W p_T below the jet p_T threshold (> 20 GeV) become large (40-100%) in the one and two inclusive jet multiplicity bins, and NLO calculations near and below this threshold are not expected to perform well. Comparisons with Sherpa show similar behaviour to NLO Blackhat, HEJ also shows good agreement with the data across the full range of the measurement.

Figure 2 shows the dijet invariant mass distributions (formed from the two highest p_T jets) in the two jet and three jet inclusive multiplicity bins in comparison with theoretical predictions. Modelling of the invariant mass distribution of the two hardest jets in inclusive $W + 2$jet events and accurate accounting for the kinematic correlations of the jets is important for searches for new physics. Measurement of this variable allows for a cross-check of these dijet correlations in tuning of Monte Carlo generators and is an important validation tool for theoretical predictions that are used to describe such distributions in the search for new physics. Good agreement is seen between all three theoretical approaches and data. Slightly larger 2-jet production rates are predicted by Blackhat than are observed, but no significant shape deviations are observed in Sherpa, HEJ or NLO Blackhat.

Measured differential production cross-sections as a function of the rapidity of the n^{th} p_T-ordered jet in $W + (n)$jet inclusive events are shown in Figure 3. Data and theory are consistent in the central rapidity region within the combined experimental and systematic uncertainties. At high jet rapidities, production cross-sections tend to be overestimated in NLO Blackhat+Sherpa and standalone Sherpa, with HEJ providing a better description of the forward jets.

Figure 4 shows the probability for additional jet emission (above a threshold of 20 GeV) in inclusive $W + 2$jet events is studied as a function of dijet rapidity separation in three configurations:

1. Rapidity separation between the two hardest jets
2. Rapidity separation between the two hardest jets with an additional requirement that the additional jet be emitted into the rapidity gap defined by the rapidity interval between the two hardest jets
3. Rapidity separation of the most forward/backward jets

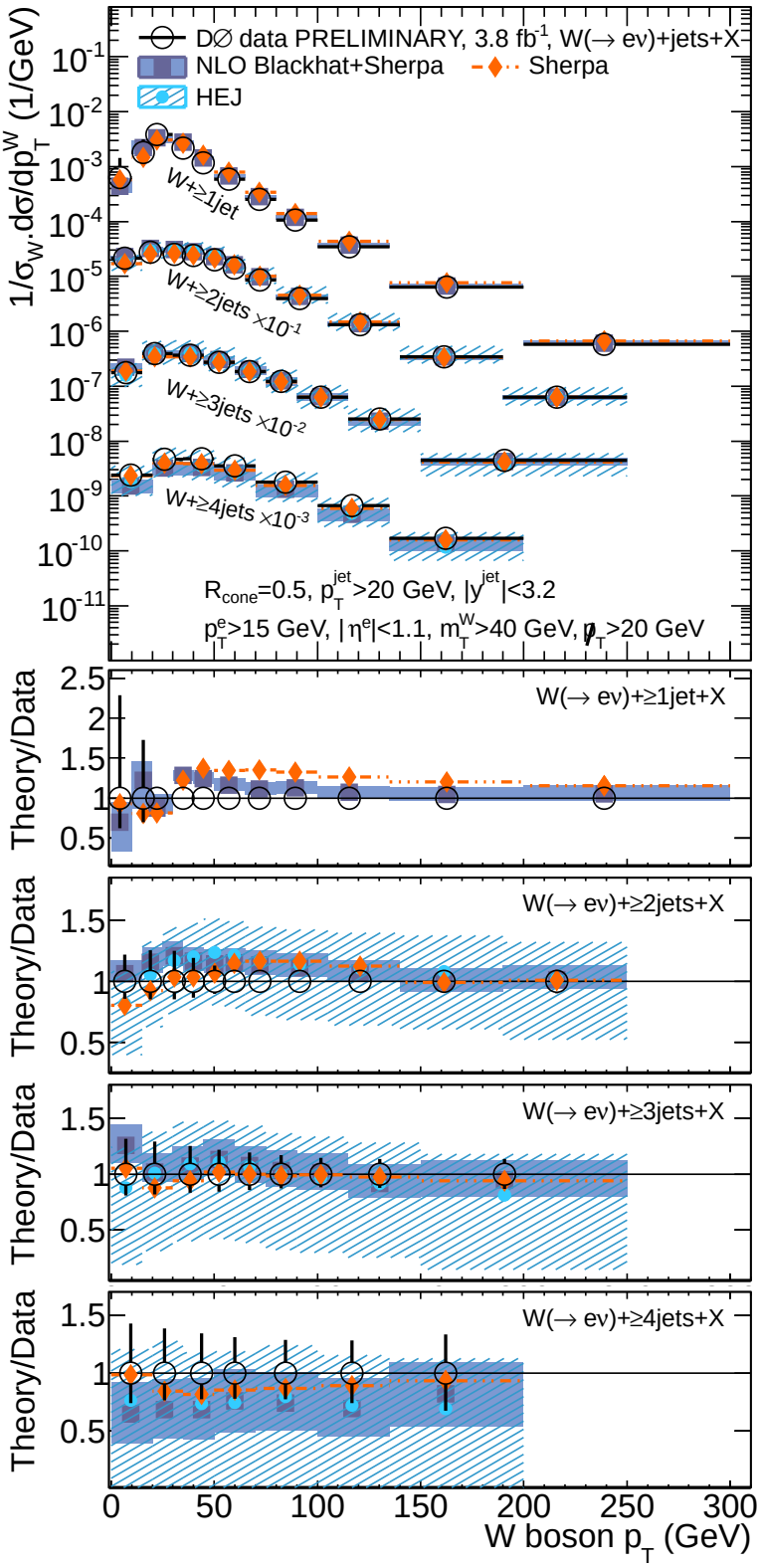

FIG. 1: Unfolded differential production cross-sections measured as a function of W boson p_T in inclusive $W + n$jet events, normalized to the measured inclusive W production cross-section. Comparison is made to NLO BLACKHAT+SHERPA predictions, HEJ all-order resummation predictions and Sherpa matrix element parton shower matched Monte Carlo predictions. Lower panes show Theory/Data ratios for each of the n-jet multiplicity bin results separately.

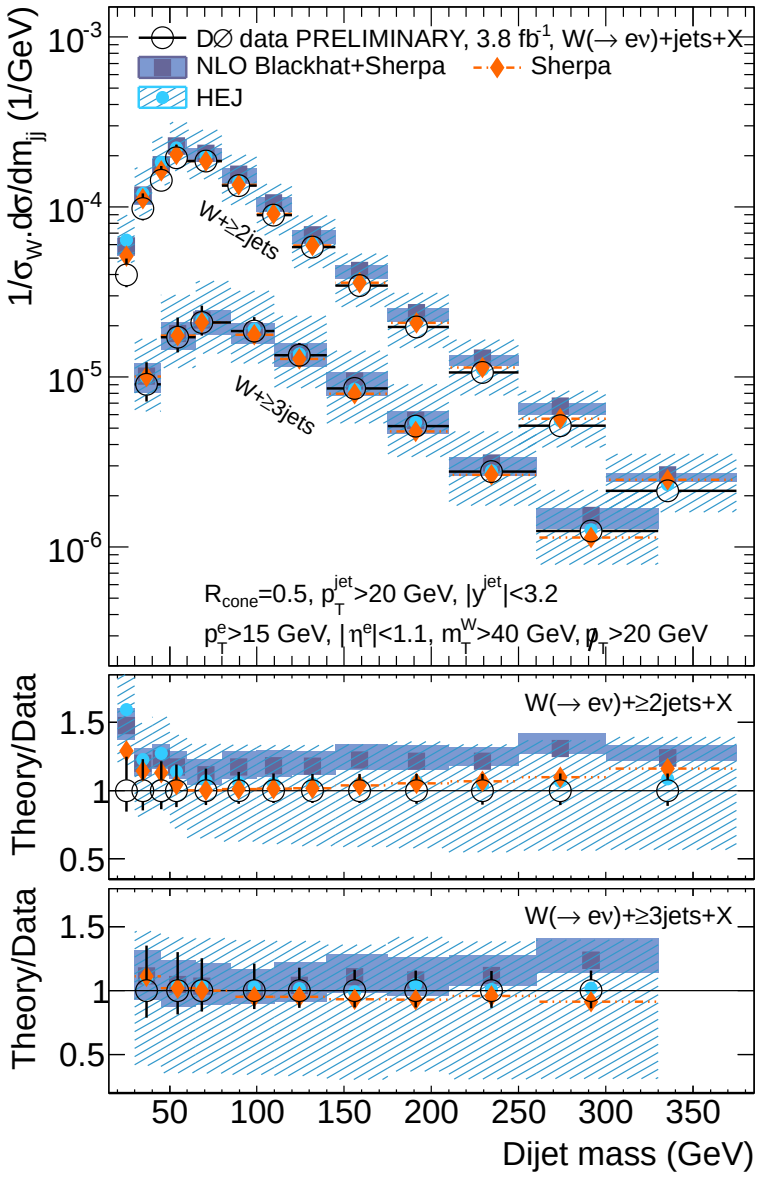

FIG. 2: Unfolded differential production cross-sections measured as a function of the invariant mass of the two highest p_T jets in inclusive $W+2$jet and $W+3$jet events, normalized to the measured inclusive W production cross-section. Comparison is made to NLO BLACKHAT+SHERPA predictions, HEJ all-order resummation predictions and Sherpa matrix element parton shower matched Monte Carlo predictions. Lower panes show Theory/Data ratios for each of the n-jet multiplicity bin results separately.

and the results shown in Figure 4 in comparison with theoretical predictions.

The first case has no additional requirement on where the third jet is emitted, so the jet emission probability is relatively constant in line with theoretical predictions, starting at around a 15% probability of further hard jet emission in inclusive W+jet events. Sherpa, HEJ and NLO Blackhat are all able to describe the data well in this configuration, with Sherpa slightly underestimating the rate of jet emission, particular at larger rapidity intervals.

The second case adds a requirement on where the third jet can be emitted. This distribution, with jets in a p_T-ordered configuration, is sensitive to wide-angle soft gluon emission. It is necessarily zero when the jets have no separation in rapidity given the absence of phase space to emit a third jet and shows a constant rise in emission probability as the phase space increases until necessarily bounded (by definition; within experimental uncertainties) from above by the p_T-ordered result without the rapidity requirement. Theoretical predictions also perform well at

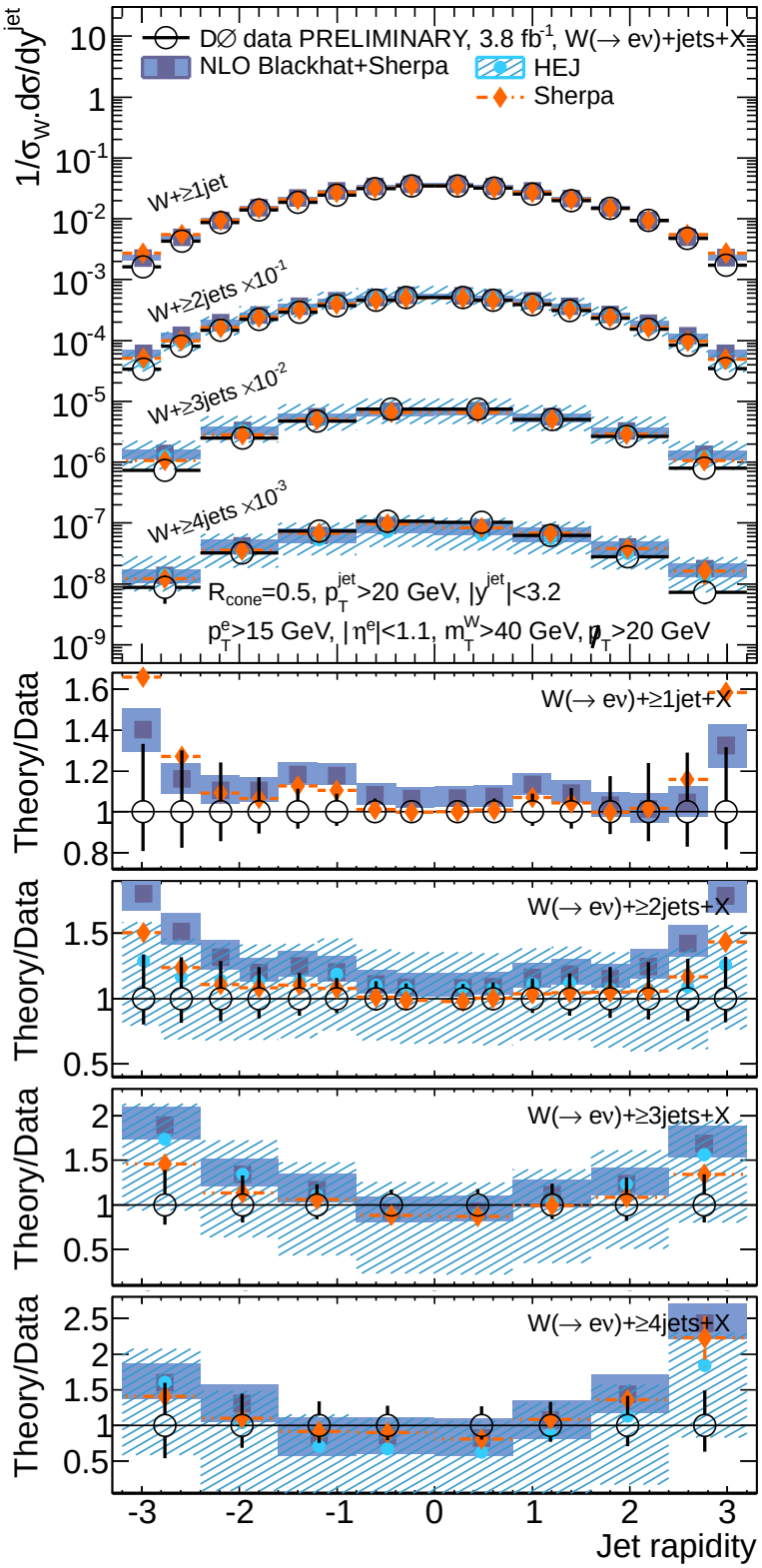

FIG. 3: Unfolded differential production cross-sections measured as a function of n^{th} jet rapidities in inclusive $W+n$jet events, normalized to the measured inclusive W production cross-section. Comparison is made to NLO BLACKHAT+SHERPA predictions, HEJ all-order resummation predictions and Sherpa matrix element parton shower matched Monte Carlo predictions. Lower panes show Theory/Data ratios for each of the n-jet multiplicity bin results separately.

describing this scenario.

The third case is an analogue of the second case but for rapidity-ordered jets, where rapidity intervals are generally larger, leading to stronger correlations and the ability to measure experimentally jet emission probabilities up to the highest rapidity separations. Any additional jet in $W + 2$jet events in this configuration will be emitted by definition into the rapidity gap defined by the most forward and backward jets, and no specific requirement on the location of the third jet emission is required. The data shows a strong correlation of emission probability, with 0% at zero rapidity gap (by definition), to around a 50% probability of emission at the largest rapidity separation. There is some indication that suppression of this jet emission rate begins to occur at the highest rapidity spans probed in this analysis with the jet emission probability evolution beginning to diverge from an otherwise linear trend despite the increasing available phase space. In this rapidity-ordered scenario, striking differences are observed between the theoretical predictions, with Sherpa diverging from the data above rapidity intervals of 3, plateauing at a emission probability of around 35%, significantly below the 50% observed in data. NLO Blackhat also begins to show some departure from the data at higher rapidity separations, with significantly increasing scale uncertainties as the spans become larger. HEJ shows agreement across the full range, with small scale uncertainties even at the highest rapidity separations.

From these results it can be seen that the rate of emission of a third jet in $W + 2$jet inclusive events is large (in p_T or rapidity ordered configurations), and that by studying the rapidity separation as a function of the most forward/backward jets, the rate of emission becomes significantly larger at even relatively modest ($\Delta y > 2$) separations, becoming around 4-5 times larger at the highest rapidity separations studied. A large emission probability for vector boson plus jet events is needed for the effectiveness of the proposed central jet veto one would wish to use to discriminate multijet and V+jet events from those with central colour singlet exchange and forward (high rapidity separated) jets for new physics searches. For these studies, Higgs searches in particular the use of as low a veto scale as possible to reduce signal event rejection is preferred, and so these results at such a low scale are particularly relevant.

These results are the first of their kind for vector boson plus jet processes, and will provide unique inputs to event generator modelling of widely separated jets and comparison and validation of different theoretical approaches to this observable, which tend to have specific and precise predictions for the evolution of the gap fraction with dijet rapidity separation.

This probability observable $\mathcal{P}$ can be reinterpreted as a measure of the gap fraction $\mathcal{F} = 1 - \mathcal{P}$ (fraction of $W + 2$jet events with a rapidity separation interval of given size) with a veto scale $Q_0 = 20$ GeV on the production of additional hard jets. Measurement of this gap fraction was recently performed by the ATLAS Collaboration in inclusive dijet studies [14] with the same veto scale. Qualitatively similar behaviours in comparison to theoretical predictions as seen in those inclusive dijet studies are observed in this analysis.

VI. CONCLUSION

Events containing jets produced in association with a W boson were studied in proton antiproton collisions at $\sqrt{s} = 1.96$ TeV with the DØ detector using 3.8 fb^{-1} of integrated luminosity. Differential production cross-section measurements, corrected to particle-level, are made of the W boson transverse momentum and n^{th} jet rapidities in $W + n$jet events (for $n = 1 - 4$), and of the invariant mass distribution of the two hardest jets in $W + 2$jet and $W + 3$jet events. In addition, in $W + 2$jet inclusive events, we study the corrected third jet emission probability as a function of the dijet rapidity separation of the two leading p_T jets (with and without the requirement that the third jet be emitted into the rapidity gap between the two leading jets) and as a function of the most rapidity separated jets. Comparison is made of these observables to predictions from all-order resummation calculations from High Energy Jets (HEJ), Next-to-Leading-Order BLACKHAT+SHERPA predictions, and predictions from the Sherpa MEPS Monte Carlo event generator. Good agreement between NLO Blackhat and the unfolded data is found although some areas involving forward jets were not perfectly described. HEJ is found to provide an accurate description of the measured observables, with high precision and accuracy in modelling wide-angle jet emission. Agreement between Sherpa and data is found to be reasonable, although areas are identified where modelling must be improved.

The authors would like to thank the BLACKHAT collaboration for providing BLACKHAT+SHERPA NLO predictions, Stefan Höche for SHERPA predictions, Tuomas Hapola and Jeppe Andersen for HEJ predictions, and Vato Kartvelishvili for useful discussions and advice on use of the GURU unfolding program.

We thank the staffs at Fermilab and collaborating institutions, and acknowledge support from the DOE and NSF (USA); CEA and CNRS/IN2P3 (France); MON, Rosatom and RFBR (Russia); CNPq, FAPERJ, FAPESP and FUNDUNESP (Brazil); DAE and DST (India); Colciencias (Colombia); CONACyT (Mexico); NRF (Korea); FOM (The Netherlands); STFC and the Royal Society (United Kingdom); MSMT and GACR (Czech Republic); BMBF

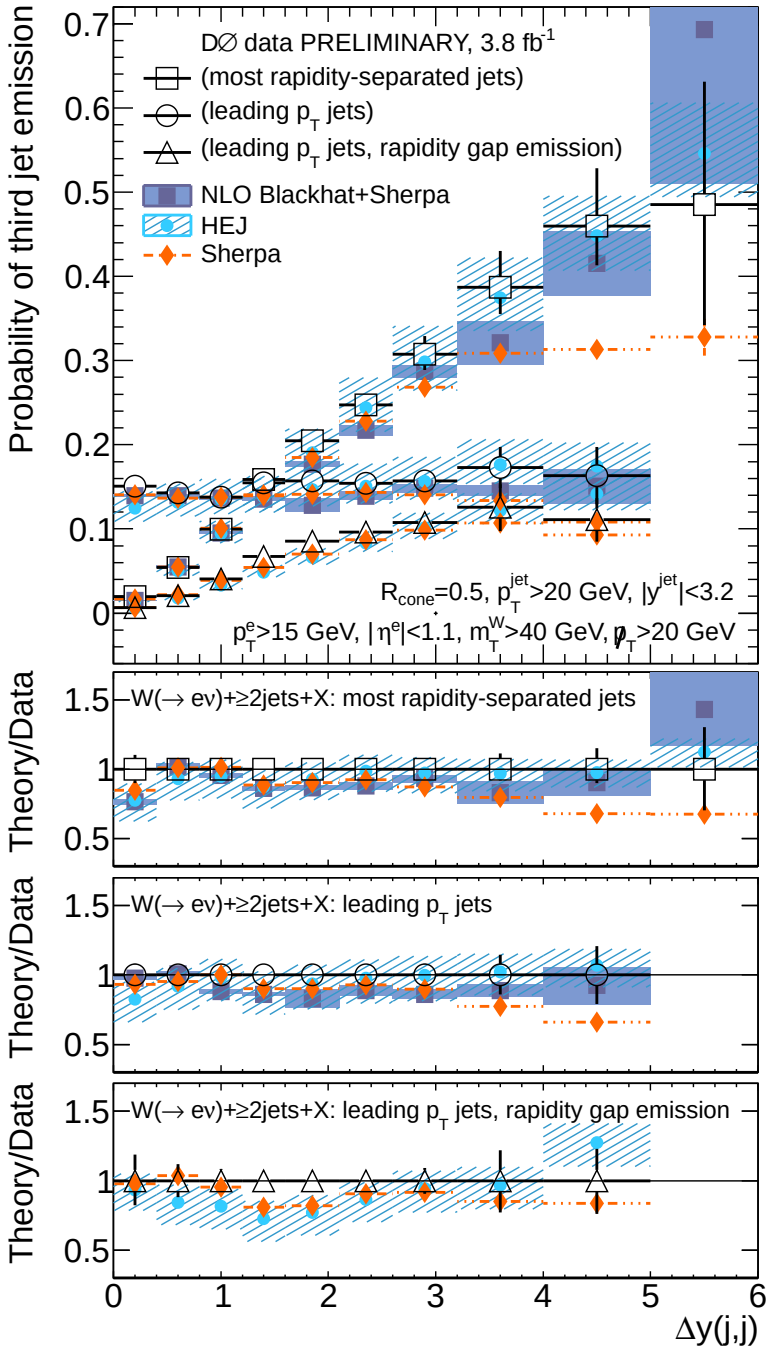

FIG. 4: Measurement of the probability of emission of a third jet in inclusive $W+2$jet events as a function of the dijet rapidity separation of (a) the two most rapidity separated jets (still above a p_T threshold of 20 GeV), (b) the two leading p_T jets, (c) the two leading p_T jets with a requirement that the third jet be emitted into the rapidity gap defined by the two leading jets. These results can also be reinterpreted as a measure of the gap fraction (fraction of $W+2$jet events with a rapidity gap of given size) with veto scale $Q_0 = 20$ GeV. Comparison is made to NLO BLACKHAT+SHERPA predictions, HEJ all-order resummation predictions and Sherpa matrix element parton shower matched Monte Carlo predictions.

and DFG (Germany); SFI (Ireland); The Swedish Research Council (Sweden); and CAS and CNSF (China).

[1] V.M. Abazov *et al.*, (D0 Collaboration), "The upgraded DØ detector," Nucl. Instrum. Methods Phys. Res. A **565**, 463 (2006).
[2] V. M. Abazov *et al.* [D0 Collaboration], "Measurements of inclusive W+jets production rates as a function of jet transverse momentum in $p\bar{p}$ collisions at $\sqrt{s} = 1.96$ TeV," Phys. Lett. B **705**, 200 (2011) [arXiv:1106.1457 [hep-ex]].
[3] J. R. Forshaw, A. Kyrieleis and M. H. Seymour, "Gaps between jets in the high energy limit," JHEP **0506** (2005) 034 [hep-ph/0502086]; J. Forshaw, J. Keates and S. Marzani, "Jet vetoing at the LHC," JHEP **0907** (2009) 023 [arXiv:0905.1350 [hep-ph]].
[4] J. R. Andersen and J. M. Smillie, "Constructing All-Order Corrections to Multi-Jet Rates," JHEP **1001** (2010) 039 [arXiv:0908.2786 [hep-ph]].
[5] G. C. Blazey *et al.*, in *Proceedings of the Workshop: QCD and Weak Boson Physics in Run II,* edited by U. Baur, R.K. Ellis, and D. Zeppenfeld, Fermilab-Pub-00/297 (2000).
[6] A. Hocker and V. Kartvelishvili, "SVD approach to data unfolding," Nucl. Instrum. Meth. A **372** (1996) 469 [hep-ph/9509307].
[7] J. R. Andersen and J. M. Smillie, "High Energy Description of Processes with Multiple Hard Jets," Nucl. Phys. Proc. Suppl. **205-206** (2010) 205 [arXiv:1007.4449 [hep-ph]]; J. R. Andersen and J. M. Smillie, "Multiple Jets at the LHC with High Energy Jets," JHEP **1106**, 010 (2011) [arXiv:1101.5394 [hep-ph]].
[8] C. F. Berger, Z. Bern, L. J. Dixon, F. Febres Cordero, D. Forde, T. Gleisberg, H. Ita and D. A. Kosower *et al.*, "Precise Predictions for $W + 3$ Jet Production at Hadron Colliders," Phys. Rev. Lett. **102** (2009) 222001 [arXiv:0902.2760 [hep-ph]]; C. F. Berger, Z. Bern, L. J. Dixon, F. Febres Cordero, D. Forde, T. Gleisberg, H. Ita and D. A. Kosower *et al.*, "Multi-jet cross sections at NLO with BlackHat and Sherpa," arXiv:0905.2735 [hep-ph].
[9] T. Gleisberg, S. .Hoeche, F. Krauss, M. Schonherr, S. Schumann, F. Siegert and J. Winter, "Event generation with SHERPA 1.1," JHEP **0902** (2009) 007 [arXiv:0811.4622 [hep-ph]].
[10] H. -L. Lai, M. Guzzi, J. Huston, Z. Li, P. M. Nadolsky, J. Pumplin and C. -P. Yuan, "New parton distributions for collider physics," Phys. Rev. D **82** (2010) 074024 [arXiv:1007.2241 [hep-ph]].
[11] S. Hoeche, F. Krauss, S. Schumann and F. Siegert, "QCD matrix elements and truncated showers," JHEP **0905** (2009) 053 [arXiv:0903.1219 [hep-ph]].
[12] T. Aaltonen *et al.* [CDF Collaboration], "Studying the Underlying Event in Drell-Yan and High Transverse Momentum Jet Production at the Tevatron," Phys. Rev. D **82** (2010) 034001 [arXiv:1003.3146 [hep-ex]] (Rivet-ID CDF_2010_S8591881_DY).
[13] A. D. Martin, W. J. Stirling, R. S. Thorne and G. Watt, "Parton distributions for the LHC," Eur. Phys. J. C **63** (2009) 189 [arXiv:0901.0002 [hep-ph]].
[14] ATLAS Collaboration, "Measurement of dijet production with a veto on additional central jet activity in pp collisions at sqrt(s)=7 TeV using the ATLAS detector," JHEP **1109** (2011) 053 [arXiv:1107.1641 [hep-ex]].